Journal of Statistical Physics, Vol. 73, Nos. 1/2, 1993

Study of the Three-Dimensional Ising Model on Film Geometry with the Cluster Monte Carlo Method

C. Ruge,[1] S. Dunkelmann,[1] F. Wagner,[1] and J. Wulf[1]

Received December 17, 1992; final March 10, 1993

Topological properties of clusters are used to extract critical parameters. This method is tested for the bulk properties of $d=2$ percolation and the $d=2, 3$ Ising model. For the latter we obtain an accurate value of the critical temperature $J/k_B T_c = 0.221617(18)$. In the case of the $d=3$ Ising model with film geometry the critical value of the surface coupling at the special transitions is determined as $J_{1c}/J = 1.5004(20)$ together with the critical exponents $\beta_1^m = 0.237(5)$ and $\phi = 0.461(15)$.

KEY WORDS: $d=3$ Ising model; cluster algorithm; critical temperature; finite-size scaling; surface-related critical exponents.

1. INTRODUCTION

The critical behavior of magnetic materials with variable strenght of coupling on the surface is characterized by surface critical exponents independent of the bulk exponents. For their theoretical determination ε-expansion,[1] series expansion,[2] and Monte Carlo methods[3,4] were applied. The latter are made conveniently using a $d=3$ Ising model embedded in a film geometry. In ref. 3 it is shown that using the Monte Carlo method critical parameters can be determined with comparable or higher accuracy as compared with other methods. In this paper we report on Monte Carlo simulations of the same model using an improved method: the cluster algorithm. This will lead to a considerable gain in accuracy.

We consider Ising spins σ_x defined on the sites x of a d-dimensional cubic lattice with periodic boundary conditions in $d-1$ directions and two free surfaces in the remaining direction (so-called film geometry). If we take the nearest-neighbor coupling J_1 in the surface layers different from the

[1] Institut für Theoretische Physik und Sternwarte, Universität Kiel, D-2300 Kiel, Germany. E-mail: pas11@rz.uni-Kiel.dbp.de.

0022-4715/93/1000-0293$07.00/0

bulk coupling J, we get the following expression for the energy of a spin configuration:

$$E = -J \sum_{(x,\mu)\notin A} \sigma_x \sigma_{x+\mu} - J_1 \sum_{(x,\mu)\in A} \sigma_x \sigma_{x+\mu} \tag{1.1}$$

The second sum runs over all surface links (x, μ) which are excluded in the first. A schematic phase diagram[5] in the J_1/J, T plane is depicted in Fig. 1. For temperatures approaching the bulk critical value T_c from above the bulk can order either with a paramagnetic surface (ordinary transition at small J_1/J) or in the presence of an already ordered surface (extraordinary transition at large J_1/J). Both regions are separated by a multicritical region (special transition at J_{1c}/J). In each region the surface magnetization is characterized by its own critical exponent β_1. Near the special transition there is an additional anomalous dimension $-\phi/\nu$ for the surface coupling $(J_1 - J_{1c})/J$. The aim of this paper is to determine J_{1c}/J as well as the critical indices at the ordinary and special transitions.

In ref. 3 a local Monte Carlo method was employed. For several reasons a cluster algorithm[6,7] may improve the accuracy. Besides the considerable reduction of critical slowing down of a cluster algorithm as compared to a local algorithm, improved extimators, for example, for the susceptibility can be used. Moreover, the distribution of large (percolating) clusters exhibits the behavior expected from finite-size scaling (FSS). It has

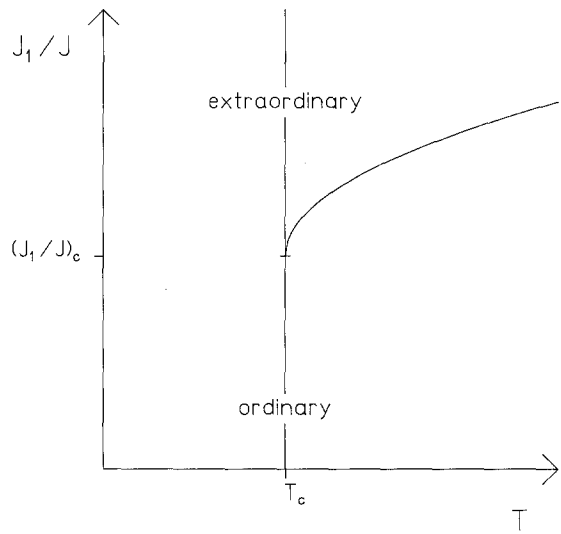

Fig. 1. The phase diagram for the $d = 3$ Ising model with film geometry in the J_1/J, $k_B T/J$ plane.

been demonstrated that bulk critical indices can be extracted from the distributions both for the Swendsen–Wang algorithm[8] and the single-cluster method.[9] Hitherto, the separation of these large clusters remained unsatisfactory. The criterion of the largest cluster in a Swendsen–Wang decomposition of the lattice used in ref. 8 cannot be applied to the computationally simpler single-cluster method. The separation in ref. 9 relies on a parametrization of the cluster size distribution. Criteria based on percolation usually require free surfaces, which leads to a slow approach to the inifinite system. In this paper we use a topological property of the large clusters. Within periodic boundary conditions a loop number l is assigned to a cluster if it contains a set of sites allowing paths going around the torus in l independent directions. Only the large clusters can contribute to $l \neq 0$. The percolating cluster, which appears at the transition into the ordered phase, has $l = d$ on a large but finite lattice. Our main observation is that the anomalous dimensions in FSS of cluster observables are independent of the loop number $l \neq 0$. A similar observation has been made for clusters defined as regions of equal spins in ref. 10. Therefore ratios of observables with different l can depend in the scaling region only on dimensionless variables such as the ratio of lattice size L to correlation length ξ. At $T = T_c$ the ratio L/ξ vanishes independent of L, leading to a determination of an unknown T_c. Such dimensionless ratios can be formed by a suitable combination of n-point functions also for spin variables (e.g., the fourth-order cumulant of the order parameter as advocated in ref. 11). However, n-point functions including the disconnected parts are almost constant, whereas connected ones are difficult to determine. We shall demonstrate that moments of the cluster size distribution exhibit enough variation to allow an accurate determination of T_c.

Before we apply our method to the surface problem mentioned above we will test it in cases where either exact or sufficiently accurate results are available. For this purpose we select $d = 2$ bond percolation[12] and the Ising model in $d = 2, 3$[13] dimensions, all with periodic boundary conditions (hereafter abbreviated by p.b.c.).

The paper is organized as follows. In Section 2 the cluster algorithms are summarized and the necessary modifications in the case of a surface problem are given. Section 3 contains the description of the method to extract critical parameters and the results for the known models. In Section 4 we report on the new results for the critical parameters at the ordinary and special transitions for the $d = 3$ Ising model with film geometry. We also discuss possible violations of FSS. Some of the results independent of scaling violations are published in a letter.[14] Section 5 contains our concluding remarks.

2. CLUSTER ALGORITHM

We use a d-dimensional sc lattice with either periodic boundary conditions or film geometry. In the first case we have $V = L^d$ sites and in the second case A surface points are contained in the total number of sites $V = \frac{1}{2}AL$. First we discuss the cluster algorithm with no surfaces. The generalization to film geometry will be given later.

The models considered here are special cases of a Q-state Potts model (see, e.g., ref. 15). Each spin σ_x can take Q different values. The bulk part of the energy is given by

$$E = -JQ \sum_{x,\mu} \delta_{\sigma_x, \sigma_{x+\mu}} \tag{2.1}$$

$Q = 2$ amounts to the Ising case and extrapolation to $Q = 1$ describes the bond percolation.[12] One is interested in averages of an observable O in thermal equilibrium

$$\langle O \rangle = \frac{1}{Z} \sum_{\{\sigma\}} O(\sigma) \exp\left(-\frac{1}{k_B T} E\right) \tag{2.2}$$

where Z is given by $\langle 1 \rangle = 1$. In order to simulate the sum (2.2) with the algorithm of Swendsen and Wang[6] (hereafter abbreviated by SW), a sequence of configurations is generated in two steps. First all the links (x, μ) of the lattice are activated according to the following probability $p(x, \mu)$:

$$p(x, \mu) = \begin{cases} 0 & \sigma_x \neq \sigma_{x+\mu} \\ 1 - \exp(-QJ/k_B T) & \sigma_x = \sigma_{x+\mu} \end{cases} \tag{2.3}$$

Sets of sites with equal spin σ connected by activated links are called clusters.

In the second step the spin value of each cluster is chosen out of the Q possible values at random. Since the cluster spins are independent, an improved estimator for the susceptibility χ at $T > T_c$ can be derived[16] (see also the Appendix):

$$\chi(T, L) = \left\{ \sum_c \frac{s_c^2}{V} \right\} \tag{2.4}$$

In (2.4) $\sum_c$ stands for a sum over clusters of one decomposition of the lattice and $\{\cdot\}$ denotes an average over different decompositions. The observable (2.4) can be generalized to the moments of the cluster distribution

$$M_n = \left\{ \sum_c \left(\frac{s_c}{V}\right)^n \right\} \tag{2.5}$$

In the $Q=1$ case thermal averages (2.2) become trivial. $p(x, \mu)$ is independent of the link, but still T dependent, and the moments (2.5) describe the usual bond percolation. In each configuration we have the identity

$$\sum_c s_c = V \tag{2.6}$$

Therefore the moments M_n are normalized to $M_1 = 1$. In the ordered phase for $T < T_c$ there exists at most one percolating cluster if the dimension is less than 6.[17] This is strictly true only in $d=2$. For $d>2$ it is generally believed that this holds to a very good approximation.[18] If we define the property Θ_{per} for this cluster on a finite lattice, the probability m_p of a site belonging to this cluster defines an order parameter for $L \to \infty$

$$m_p = \left\{ \frac{s}{V} \Theta_{\text{per}} \right\} \tag{2.7}$$

For the following we do not need the equality of (2.7) with the usual magnetization, we only require m_p having the same anomalous dimension.

In each Monte Carlo step a decomposition of the lattice into clusters is needed for the averages $\{\cdot\}$. Even though there exists an efficient algorithm for this purpose,[19] this can be avoided by the single-cluster method proposed for percolation by Leath[20] and for correlated percolation by Wolff.[7] The sum over all clusters in the single-cluster observable (2.5) is evaluated by generating only one cluster in each step using probabilities (2.3) starting at x_0. Choosing this site and its cluster with probability $q(x_0, c)$, one can replace the average (2.5) by

$$M_n = \left\langle \frac{1}{q(x_0, c)} \left(\frac{s}{V} \right)^n \right\rangle_q \tag{2.8}$$

The efficiency can be further increased[7,21] if in each spin update the cluster spins are given a random value different from the old one. The choice of $q(x_0, c)$ is restricted by the normalization condition $\sum_c q(x_0, c) = 1$ for each SW decomposition. Wolff used the identity (2.6) for the choice

$$q(x_0, c) = \frac{s_c}{V} \tag{2.9}$$

which means the starting site x_0 is chosen at random in the lattice. With (2.9) and (2.8) we get for the moments

$$M_n = \left\langle \left(\frac{s}{V} \right)^{n-1} \right\rangle \tag{2.10}$$

Here $\langle \cdot \rangle$ denotes an average over the single cluster steps [as $\langle \cdot \rangle_q$ in (2.8)]. The single-cluster method is easier to implement and can lead to higher efficiency.[7,22] Both cluster methods can also be applied to other spin models than the Q-state Potts model.[16,21] In this case relation (2.4) between the moment M_2 and the usual susceptibility does no longer hold.[23]

In relation (2.7) for the order parameter we need an estimator for the infinite cluster on a finite lattice. With periodic boundary condition we can assign a loop number l ($0 \leqslant l \leqslant d$) to each cluster, which means that inside the cluster at least l paths exist going around the torus in l independent directions. The property for these clusters is denoted by Θ_l. Examples are given in Fig. 2 for a 3×3 lattice in $d = 2$.

Only clusters with loop number d can contribute to the order parameter (2.7), since in the limit $\xi/L \to 0$ for $T < T_c$ there exist only finite clusters and the percolating cluster. Therefore we estimate m_p by

$$m_p = \left\{ \frac{s}{V} \Theta_d \right\} = \langle \Theta_d \rangle \tag{2.11}$$

With the help of Θ_l we can also measure the size distribution of clusters with loop number l, which is expressed by the moments

$$M_n(\Theta_l) = \left\{ \sum_c \left(\frac{s_c}{V} \right)^n \Theta_l \right\} = \left\langle \left(\frac{s}{V} \right)^{n-1} \Theta_l \right\rangle \tag{2.12}$$

The advantage of moments (2.12) with $l \neq 0$ over the moments in (2.5) is their higher sensitivity to large clusters. Therefore they approach the scaling limit faster. Since $\sum_l \Theta_l = 1$, the moments (2.5) can be expressed by (2.12).

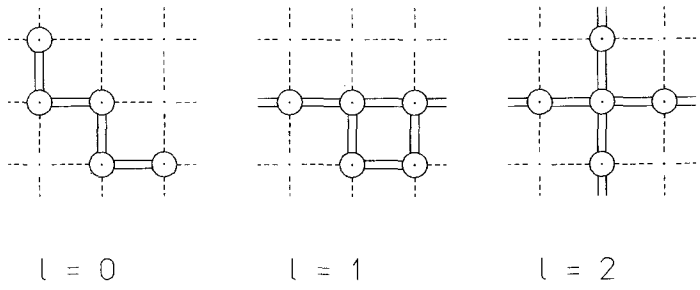

Fig. 2. Examples of $s = 5$ clusters in a 3×3 p.b.c. lattice with different loop numbers. The sites of the clusters are denoted by $\odot$ and links belonging to the cluster by double lines.

We now turn to the modifications and generalizations implied by the presence of a surface. The SW algorithm has to be modified in such a way that on the r.h.s. of (2.3) the interaction strength J is replaced by J_1 for links in the surface. The loop number l in Θ_l can vary over $l=0,\ldots, d-1$. In addition there is the property Θ_{lp} for clusters having sites in both surfaces. Since each cluster may contain t_c surface sites, we can define the moments

$$M_{nm}(\Theta)=\left\{\sum_c \left(\frac{s_c}{V}\right)^{n-m}\left(\frac{t_c}{A}\right)^m \Theta\right\} \tag{2.13}$$

where Θ may be any property chosen from 1, Θ_l, Θ_{lp}. Within the single-cluster method the moments (2.13) are given by

$$M_{nm}(\Theta)=\left\langle\left(\frac{s}{V}\right)^{n-m-1}\left(\frac{t}{A}\right)^m \Theta\right\rangle \tag{2.14}$$

Due to the identity

$$\sum_c t_c = A \tag{2.15}$$

the moments M_{nm} are normalized to $M_{10}(1)=M_{11}(1)=1$. Equation (2.15) allows also a modification of the Wolff method. Choosing the probability $q(x_0, c)=t_c/A$ implies that the single-cluster algorithm starts anywhere in the surface. Denoting these averages by $\langle\cdot\rangle_A$, we can express the moments $M_{nm}(\Theta)$ also by the surface cluster method or

$$\left\langle\left(\frac{s}{V}\right)^{n}\left(\frac{t}{A}\right)^{m-1}\Theta\right\rangle_A=\left\langle\left(\frac{s}{V}\right)^{n-1}\left(\frac{t}{A}\right)^{m}\Theta\right\rangle \tag{2.16}$$

Due to (2.16) we do not get new information by this method. However, the statistics on surface quantities can be improved. Using only clusters starting in the surface will lead to a poor description of thermal equilibrium in the bulk. Thus we will use both kinds of starting points in equal amount. As in the bulk case, the surface susceptibilities in the disorded phase can be expressed in terms of the moments $M_{nm}(1)$:

$$\chi_1=\frac{1}{A}\sum_{x\in V,\, y\in A}\langle\sigma_x\sigma_y\rangle=\frac{1}{A}\left\{\sum_c t_c s_c\right\}=VM_{21}(1) \tag{2.17}$$

The details are given in the Appendix.

3. DETERMINATION OF CRITICAL PARAMETERS

In previous investigations[8,9] it has been shown that the large clusters exhibit a behavior expected from FSS. Let us first discuss the implications of FSS for the bulk moments (2.12). If s/V also becomes a scaling variable with anomalous dimension y_s, we expect the following behavior of the moments near the critical point T_c:

$$M_n(T, L, \Theta_l) = L^{y_{sw}+ny_s}\bar{M}_n(\Theta_l, z) \tag{3.1}$$

where y_{sw} describes the dimension of the SW distribution and z is a scale-invariant variable, for which we take

$$z = \left(\frac{T}{T_c} - 1\right) L^{1/\nu} \tag{3.2}$$

We prefer (3.2) to the usual Fisher variable ($\equiv |z|^{\nu}$), because it keeps track of the sign of $T - T_c$. Furthermore, it will turn out that the functions $\bar{M}$ and their ratios can be parametrized in most cases by either linear or exponential functions in z, which would become complicated using $|z|^{\nu}$. As in ref. 9, y_s and y_{sw} can be expressed in terms of the known dimensions of M_2 ($=\chi/V$) and the order parameter (2.11), which gives

$$y_{sw} = 0$$

$$y_s = -\beta/\nu$$

The scaling law (3.1) applies only to moments sensitive to large clusters, which means $M_n(\Theta_0)$ has to be excluded for $n < 2$. If we take ratios of $M_n(\Theta_l)$ with different l

$$r_n(\Theta_l, \Theta_{l'}, z) = \frac{M_n(\Theta_l)}{M_n(\Theta_{l'})} \tag{3.3}$$

we have observables which can depend on z only. Equation (3.3) provides an easy way to locate an unknown T_c. If r_n is plotted as a function of T for different L, r_n becomes independent of L at $T = T_c$ (or $z = 0$). With T_c known, a value for ν follows from the requirement that for different L the ratio r_n should lie on the same universal curve as a function of z. Finally, β/ν can be determined from the variation of M_n at $z = 0$:

$$M_n(\Theta_l, L)_{T=T_c} = L^{-n\beta/\nu}\bar{M}_n(\Theta_l, 0) \tag{3.4}$$

The method works only if the moments vary in the critical region at all. This is expected, since in the limit $z \to \infty$ we get no clusters with loop

number $l \neq 0$, whereas in the limit $z \to -\infty$ a finite fraction of clusters with $l = d$ must be present. Therefore at least $r_n(\Theta_0, \Theta_d, z)$ has to show a substantial variation crossing the critical point at $z = 0$.

The first model we want to test is $d = 2$ bond percolation. We generated 20000 clusters per point in the range of $0.495 \leqslant p \leqslant 0.505$ with $p = 1 - \exp(-J/k_B T)$. In Fig. 3 the ratio

$$r(p, L) = \frac{M_1(\Theta_2)}{M_1(\Theta_1)} \tag{3.5}$$

is shown as a function of p for different lattice sizes L, which obviously have a common point of intersection. From a linear fit to $\ln r$ we obtain the critical value of p:

$$p_c = 0.49996(11) \tag{3.6}$$

close to the theoretical value 1/2.[12] With $p_c = 1/2$ the same data are shown in Fig. 4 as a function of $z \equiv (p_c - p)L^{1/\nu}$, where $1/\nu$ is fitted together with a straight line to $\ln r(z)$, to obtain the best scaling behavior:

$$\nu = 1.37(5) \tag{3.7}$$

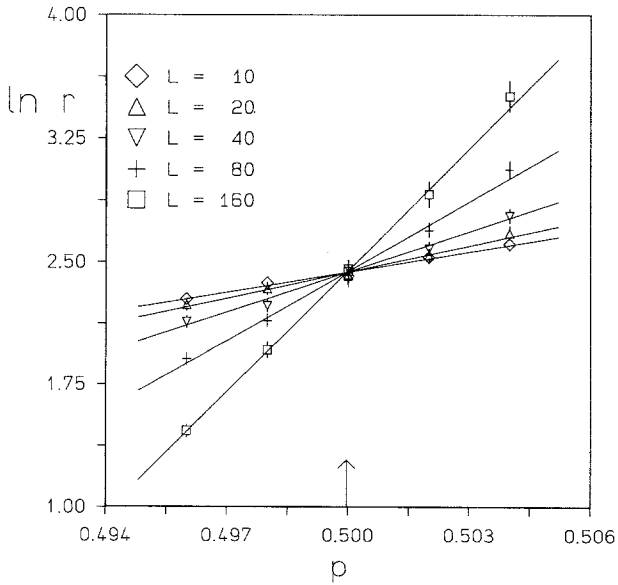

Fig. 3. Plot of $\ln r$, with r defined as the moment ratio (3.5) for $d = 2$ bond percolation, as a function of p for different lattice sizes. The lines represent linear fits to the data. The common point of intersection gives p_c.

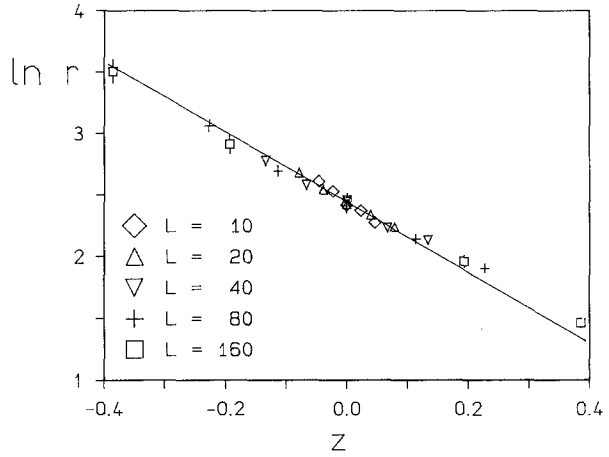

Fig. 4. The same data as in Fig. 3 shown as a function of z. If FSS holds, the data collapse into a single line. The straight line corresponds to a fit including ν as a free parameter.

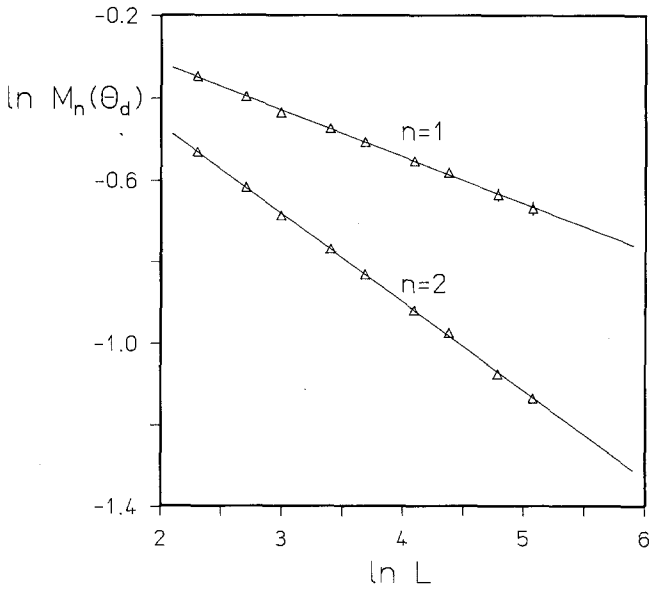

Fig. 5. Plot of ln $M_n(\Theta_2)$ at $p = p_c = 1/2$ for $d = 2$ bond percolation as a function of ln L with $n = 1, 2$. From the slopes the value (3.8) for β/ν is determined by a straight-line fit (solid lines).

The validity of FSS is obvious. Figure 5 shows the L dependence of $M_n(\Theta_2)$ at $p=p_c$ with $n=1, 2$ on a double log scale. The power law implied by (3.4) is well satisfied. From the slopes $n\beta/\nu$ in a double log plot we obtain

$$\beta/\nu = 0.104(2) \tag{3.8}$$

The values (3.7) and (3.8) are in agreement with the theoretical values, which are given in Table I. Other moments or ratios exhibit the expected behavior with less statistical significance.

Now we apply the same method to the Ising model dimensions with p.b.c. in $d=2, 3$. To determine $(k_BT/J)_c$ we typically generated 20000–100000 clusters at each value of T and L.

Figure 6 shows the most significant ratio $r=M_2(\Theta_d)/M_2(\Theta_0)$ as a function of $J/(k_BT)$ for various L. Again a common point of intersection is evident. Fitting $\ln r$ by straight lines, we obtain

$$d=2: \quad \left(\frac{J}{k_BT}\right)_c = 0.440686(10) \tag{3.9}$$

$$d=3: \quad \left(\frac{J}{k_BT}\right)_c = 0.221617(18) \tag{3.10}$$

The errors in (3.9), (3.10) include the measured autocorrelation time. The achieved accuracy is surprisingly high, considering the moderate computing effort. Our result for $d=3$ agrees with the series expansion by Liu and Fisher[24] and within 2 standard deviations with the result from the Monte Carlo renormalizations group[25,26] and the histogram method of ref. 27. The same data are shown in Fig. 7 as a function of z, including ν as a

Table I. Comparison of Critical Parameters Obtained by the Cluster Method (Values without Reference) with Values Given in the Literature

	$J/(k_BT_c)$ or p_c	ν	β/ν
Bond percolation, $d=2$	0.49996(11) $1/2$[18]	1.372(49) $4/3$[18]	0.104(2) $5/48$[18]
Ising model, $d=2$	0.440686(10) 0.4406867 ...[13]	1.001(3) 1[13]	0.126(3) $1/8$[13]
Ising model, $d=3$	0.221617(18) 0.221630(10)[24] 0221654(6)[25] 0.221658(3)[27]	0.636(5) 0.633[24]	0.516(7) 0.522[24] 0.516(6)[9]

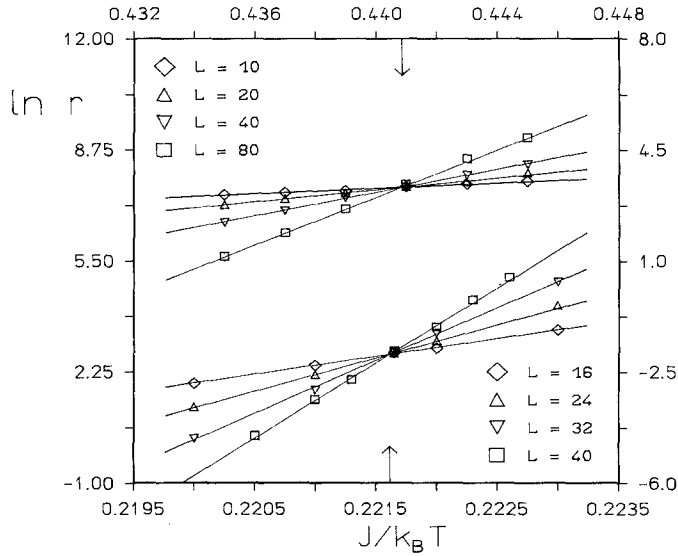

Fig. 6. Plot of $\ln r$ with $r = M_2(\theta_d)/M_2(\theta_0)$ as a function of $J/(k_B T)$ for various L for the Ising model with $d = 2$ (upper part) and $d = 3$ (lower part). The lines are fits to the data with a common point of intersection giving the values (3.10) for $J/k_B T_c$.

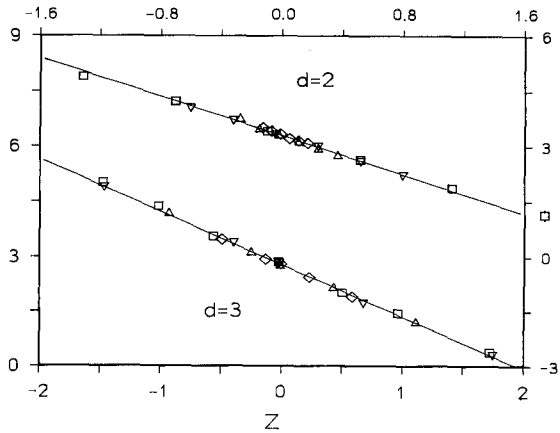

Fig. 7. Same data for $\ln r$ as in Fig. 6 as a function of $z = (T/T_c - 1)L^{1/\nu}$ for $d = 2$ and $d = 3$ Ising model. Within FSS the data should lie on the scaling curve. From the slopes of a straight-line fit a value of $1/\nu$ is obtained, giving the values of (3.11).

parameter in the straight-line fit. The ratios nicely follow the universal curve predicted by FSS with the ν values

$$\begin{aligned} d&=2 \qquad \nu=1.001(3) \\ d&=3 \qquad \nu=0.636(5) \end{aligned} \tag{3.11}$$

As in the percolation case, β/ν can be obtained from the L dependence of $M_n(\Theta_d)$ at $T=T_c$, taken from ref. 27 in the case $d=3$. Figure 8 shows M_n. The fitted slopes for $n=1, 2$ lead to

$$\begin{aligned} d&=2 \qquad \beta/\nu=0.126(3) \\ d&=3 \qquad \beta/\nu=0.516(7) \end{aligned} \tag{3.12}$$

As in the previous case, the used moments are those with the highest statistical accuracy. The critical exponents derived by other moments are compatible within the errors. Table I summarizes the comparison with other methods, which shows that using clusters with loop number different from zero leads to a reasonable accuracy for critical exponents in the tested models. In our previous investigation[9] the large clusters were separated by a parametrization of the cluster size distribution. To demonstrate the

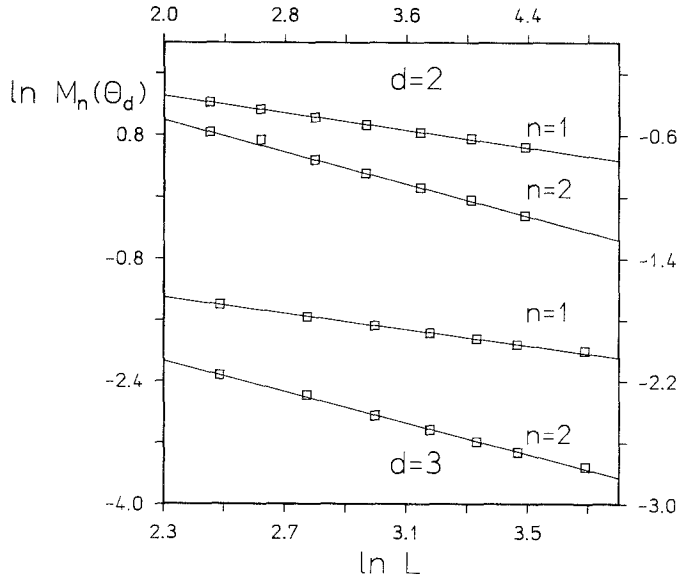

Fig. 8. The moments $\ln M_n(\Theta_d)$ at $T=T_c$ for the $d=2, 3$ Ising model with $n=1, 2$ as a function of $\ln L$. The slopes of the straight-line fits give $n\beta/\nu$.

validity of this approach, Fig. 9 shows this distribution of cluster sizes $x = s/V$ at $T = T_c$ and $L = 20$ for the $d = 3$ Ising model together with the fit of ref. 9. At low s the Θ_0-clusters dominate. The decrease with a power law is determinated by the animal exponent of percolation.[18] The peak at high s we previously assigned to the percolating cluster is completely given by Θ_3-clusters. It also shows that Θ_1- and Θ_2-clusters (which are the maximal at $T = T_c$) do not contribute significantly to the distribution.

After these tests we apply our method to the surface problem. In addition we have t/A as a scaling variable near a phase transition of the surface. Therefore in the case of special transition, scale-invariant functions can also depend on

$$z_1 = \left(1 - \frac{J_1}{J_{1c}}\right) L^{\phi/\nu} \tag{3.13}$$

The anomalous dimension y_t of t/A can be determined by the surface susceptibility (2.17) with the result

$$y_t = -\beta_1/\nu \tag{3.14}$$

If FSS applies, the moments (2.13) should scale like

$$M_{nm}(\Theta) = L^{-n\beta/\nu - m(\beta_1 - \beta)/\nu} \bar{M}_{nm}(\Theta, z, z_1) \tag{3.15}$$

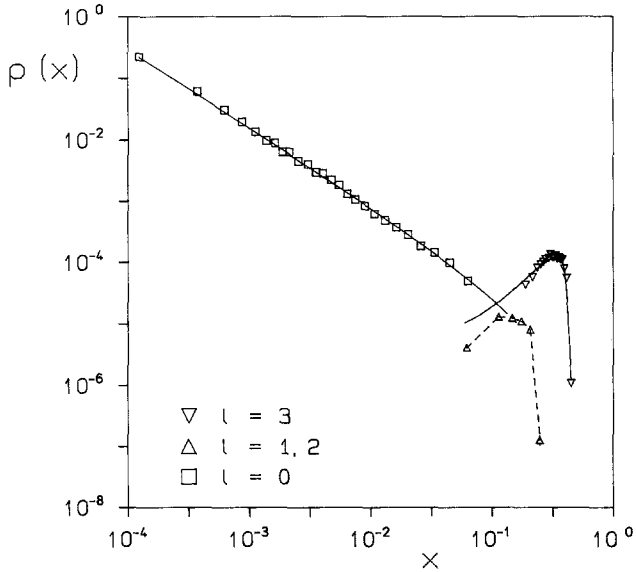

Fig. 9. The cluster size distribution $p(x)$ with $x = s/V$ of a $d = 3$ Ising model with p.b.c. and lattice size $L = 20$. The solid lines represent the contribution of finite and percolating clusters taken from the parametrization of ref. 9. The dashed line is a guide to the eye.

where Θ is one of the properties 1, Θ_l, Θ_{lp}. At the ordinary transition $\bar{M}$ is simply a function of J_1. Again (3.15) should be applied to Θ_0 or 1 only for $n \geqslant 2$. In the next section we will determine J_{1c} by dimensionless ratios and β_1 by the L or z_1 dependence at $z=0$.

In the tested models with periodic boundary conditions we found no indication for a violation of the scaling law (3.4), as already noted in ref. 9. This turned out to be different in the surface problem, where we encountered a small correction to scaling. Since we do not have a systematic way to treat these nonleading terms, we apply phenomenological formfactors in each case separately.

4. ISING MODEL WITH FILM GEOMETRY

For the area of each layer in the film geometry we have the number of surface points as $A=2L^2$, where L denotes the thickness of the film. We checked that other choices for the layer area would not change the observables if A does not differ from $2L^2$ by an order of magnitude. In the simulation we chose the starting points used by the single-cluster algorithm alternating between volume and surface. In the case of the special transition we generated 20000–100000 clusters per point at $T=T_c$ in the range $10 \leqslant L \leqslant 40$ and $1.45 \leqslant J_1/J \leqslant 1.55$. We took the value of T_c ($J/k_B T_C = 0.221165$) from ref. 27. We checked that other choices, such as our value (3.10) or the result of ref. 24, had no influence on the results of the surface quantities reported below. For the ordinary transition we generated clusters with less statistics in the same L range for $T \leqslant T_c$ and at fixed $J_1/J=0.5$.

As a test of thermalization we can check the equality (2.16) of moments obtained with volume or surface starting points. The observable χ_1 with property Θ_l can either be measured by the number t of surface cluster points per area A in the volume method or the number s of volume cluster points per volume V in the surface method. Therefore the ratios ρ_l defined by

$$\rho_l = \frac{V}{A} \frac{\langle t\Theta_l \rangle}{\langle s\Theta_l \rangle_A} \tag{4.1}$$

should be 1 in thermal equilibrium. Figure 10 shows ρ_l as a function of J_1/J for different L at $T=T_c$. The region of the multicritical point is presumably the worst case for thermalization. Inside the errors $\rho_l = 1$ holds. The same is true for other moments related by Eq. (2.16).

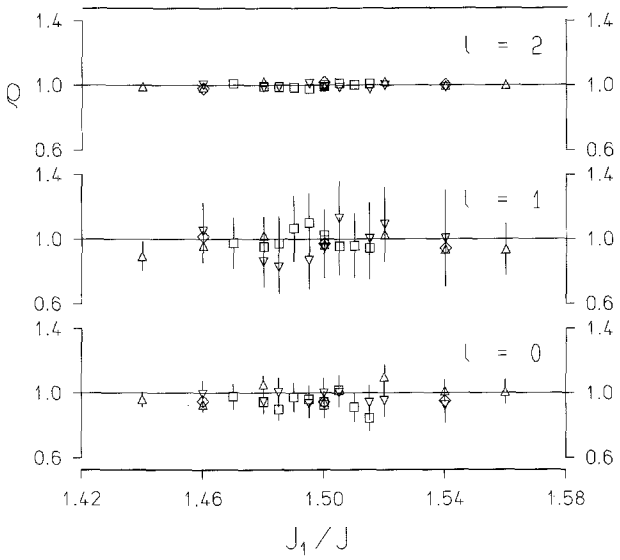

Fig. 10. Ratio ρ_l of $M_{11}(\Theta_l)$ at $T=T_c$ determined by volume and surface starting points as a function of the surface coupling near the special transition. $\diamond$, $L=10$; $\triangle$, $L=16$; ∇, $L=24$; $\square$, $L=40$. If thermal equilibrium is reached, a value of 1 is expected.

We determine the value $(J_1/J)_c$ for the multicritical point with a similar method as in Section 3. We define the following dimensionless ratio of moments at $T=T_c$:

$$r_k(z_1)=\frac{M_{2k}(\theta_{2p})}{M_{2k}(\theta_0)}=\frac{\langle s(t/s)^k\theta_{2p}\rangle}{\langle s(t/s)^k\theta_0\rangle}\bigg|_{T=T_c} \tag{4.2}$$

If FSS holds, r_k can only depend on the scaling variable $z_1=(1-J_1/J_{1c})L^{\phi/\nu}$. The ratio r_k becomes independent of L at the critical value of J_1. The data for $\ln r_1$ as a function of J_1 are shown in Fig. 11. They are compatible with a linear behavior in J_1 and a common point of intersection. From a fit indicated by the lines in Fig. 11 we obtain

$$(J_1/J)_c=1.5004(20) \tag{4.3}$$

The same data are shown in Fig. 12 as a function of z_1. The lines for different L collapse into a single curve, provided ϕ/ν is chosen as

$$\phi/\nu=0.729(15) \tag{4.4}$$

This value of ϕ/ν has been obtained by a linear fit to $\ln r_1$ (also shown in Fig. 12) including ϕ/ν as a free parameter to achieve best scaling. In

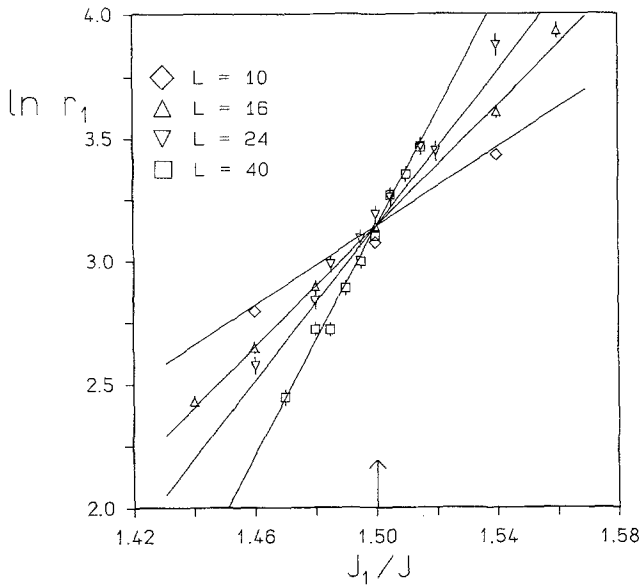

Fig. 11. Ratio $\ln r_1$, with r_1 defined as the moment ratio (4.2), as a function of J_1/J for various L at $T = T_c$. The critical J_{1c}/J is the common point of intersection. The lines are linear fits to the data.

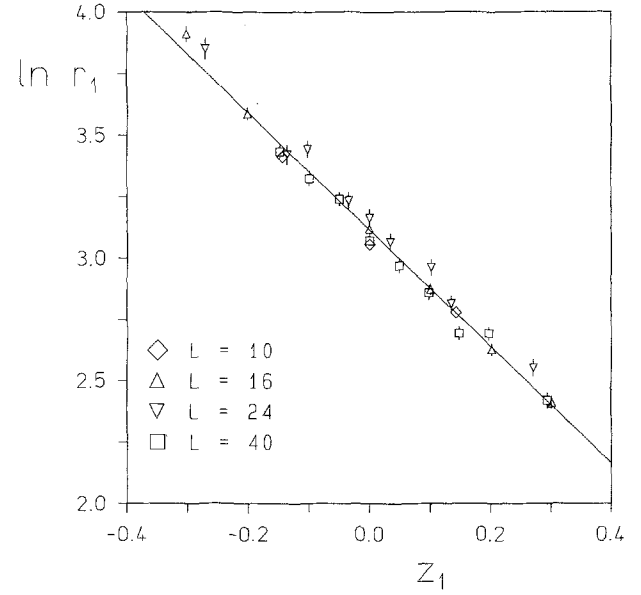

Fig. 12. The same data as in Fig. 11 as a function of $z_1 = (1 - J_1/J_{1c})L^{\phi/\nu}$. The line represents a linear fit including ϕ/ν as parameter. If FSS holds, all data should lie on the same universal curve.

Table II. Resulting Parameters in Fits to the Moment Ratios (4.3)

Used	ϕ/ν	J_{1c}/J	δ_0	δ_1	δ_2
r_1	0.729(15)	1.5004(20)	—	—	—
r_0, r_1, r_2	0.729(9)	1.5002(10)	−0.0065(2)	−0.01(3)	0.07(1)
r_0, r_1, r_2	0.740(20)	1.4991(16)	0	0	0

contrast to r_1, the ratios r_0 and r_2 exhibit a small but significant violation of scaling. This violation can be described by an additional form factor $F(\delta)$ to the theoretical expression of r_k:

$$r_k(z_1, L) = F(\delta_k, L) A_k e^{B_k z_1} \tag{4.5}$$

For F we use the form

$$F(\delta, L) = [1 + (L_0/L)^P]^{\delta/P} \tag{4.6}$$

The data are not sufficiently accurate to determine L_0 and P independently of δ. Therefore we choose $P = 2$ and $L_0 = 60$. The values of δ_k, ϕ/ν, J_1/J, and the constants A_k, B_k are free parameters in a fit to the data of $\ln r_k$. The δ_k turn out to be small (see Table II); in particular, δ_1 is compatible with zero. ϕ/ν and J_{1c}/J agree within errors with (4.3) and (4.4). Omitting the form factor at all ($\delta_k = 0$) has no consequences for the values of ϕ/ν and J_{1c}/J, but the χ^2/DOF doubles. Other moments different from (4.3) have less statistical significance. Since we need no corrections for the data of r_1, we take the result of (4.3) and (4.4) as our final values quoted in Table III. We estimate β_1 from the L dependence of the following moments at $T = T_c$:

$$M_{nk}(\theta_{2p}) = \left\langle \left(\frac{s}{V}\right)^{n-1} \left(\frac{tV}{sA}\right)^k \theta_{2p} \right\rangle \tag{4.7}$$

Table III. Comparison of Values for the Critical Parameters of the Present Work with Values Given in the Literature[a]

	J_{1c}/J	ϕ	β_1^m	β_1
Present	1.5004(20)	0.461(15)	0.237(5)	0.75(2)
Landau and Binder	1.52(2)	0.59(4)	0.18(2)	0.78(2)
Mean field (ε^0)	5/4	1/2	1/2	1
ε-Expansion linear	—	0.41	0.250	0.833
ε-Expansion quadratic	—	0.68	0.245	0.816

[a] We use $\beta = 0.330$ and $\nu = 0.633$ from ref. 24 to convert the merasured values into the values given here.

In the scaling ansatz for M_{nk} we allow a possible violation of scaling by a multiplicative formfactor as in (4.5):

$$M_{nk}(\theta_{2p}, z_1, L) = L^{k\Delta\eta - n\beta/\nu} F(\alpha_{nk}, L)\, \bar{M}_{nk}(z_1) \tag{4.8}$$

The first factor on the r.h.s. of (4.8) reflects the anomalous dimension of M_{nk}, which depends on β_1 via

$$\Delta\eta = \eta_\perp - \eta_{||} = \frac{1}{\nu}(\beta - \beta_1) \tag{4.9}$$

For $F(\alpha, L)$ we take the parametrization (4.6) again. The last factor in (4.8) contains the scale-invariant dependence on z_1. Even with known β/ν our accuracy does not allow us to extract $\Delta\eta$ from (4.8) without an assumption on the scaling violation parameter α_{nk}. If we consider cross ratios like

$$\frac{M_{n_1, k+K} M_{n_2, k-K}}{M_{n_1, k+K'} M_{n_2, k-K'}}$$

which depend at a fixed z_1 only on the ratios of formfactors like $F(\alpha_{nK,L})/F(\alpha_{nK'}, L)$, we find that those ratios are independent of K, K' (see Table IV). Therefore we assume that α_{nk} does not depend on k, which is compatible with the data at least. With this assumption (4.8) reads now

$$M_{nk}(\theta_{2p}, z_1, L) = (F(\alpha_n, L) L^{-n\beta/\nu})\, L^{k\Delta\eta} \bar{M}_{nk}(z_1) \tag{4.10}$$

The first factor on the r.h.s. of (4.10) depends on n only and allows a determination of α_n if β/ν is known. The L dependence of moments with different k determines $\Delta\eta$. If we restrict the range of z_1 to $|z_1| \leqslant 0.4$, a linear dependence on z_1 turned out to be sufficient for the scaling function $\ln \bar{M}$. In a fit to the $n=1$ moments with $k=0$, 1 and $\beta/\nu = 0.512$ we obtain

$$\alpha_1 = 0.008(6), \qquad \Delta\eta = 0.147(6) \tag{4.11}$$

Table IV. Values of Ratios of $M_{nm}(\Theta_2)$ Moments at $z = z_1 = 0$, Which Are L Independent If the Assumption (4.10) about the Formfactor Is Correct

L	$M_{10}M_{11}/M_{01}M_{20}$	$M_{11}M_{00}/M_{01}M_{10}$	$M_{00}M_{20}/M_{10}^2$	$L^{\beta/\nu}M_{10}$
10	1.32(4)	0.80(3)	0.60(3)	1.25(1)
16	1.31(5)	0.84(3)	0.64(3)	1.25(1)
24	1.28(6)	0.82(5)	0.64(4)	1.23(1)
40	1.29(5)	0.81(4)	0.63(3)	1.24(1)

and similarly for the $n=2$ moments with $k=0, 1, 2$

$$\alpha_2 = 0.065(2), \qquad \Delta\eta = 0.147(2) \tag{4.12}$$

In Fig. 13 and 14 we show the data for $M_{nk}L^{n\beta/\nu}/F(\alpha_n, L)$ and the fit for $\bar{M}_{nk}(z_1)$ as a function of z_1 for various L. The fit shows that the L dependence is adequately described by the parametrization (4.10). $\alpha_2 \neq 0$ signalizes a small violation of scaling in the moments M_{2k}, whereas the L dependence of M_{1k} is in accordance with FSS. Absence of scaling violations in M_{10} can be seen directly by $L^{\beta/\nu}M_{10}$ given in the last column of Table IV. The values (4.11) and especially (4.12) vary slightly with the values L_0 and P chosen in the parametrization (4.6) of the form factor. We can estimate a systematic error of $\Delta\eta$ by varying L_0 and P inside reasonable margins, obtaining our final value for $\Delta\eta$:

$$\Delta\eta = 0.147(8) \tag{4.13}$$

$\Delta\eta$ can be converted into a value for β_1^m using (4.9):

$$\beta_1^m = 0.237(5) \tag{4.14}$$

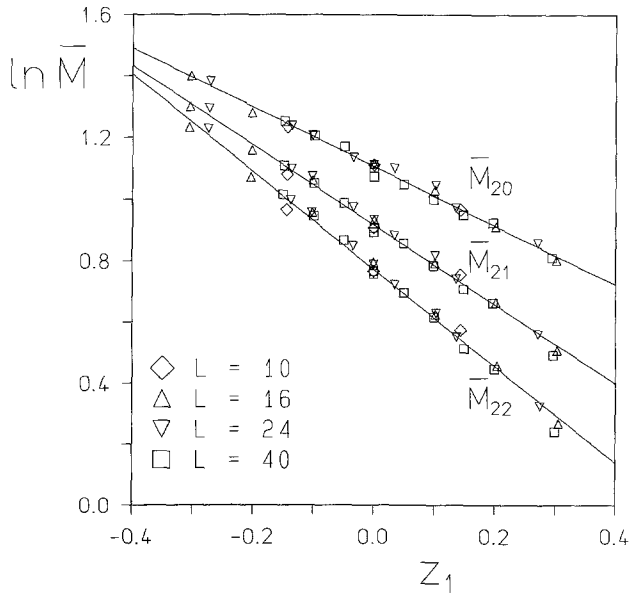

Fig. 13. Plot of $\ln \bar{M}_{2,k}(z_1)$ defined in (4.10) at $T=T_c$ as a function of z_1 for various L and $k=0, 1, 2$. The lines are linear fits to the data including $\Delta\eta$ and the formfactor as free parameters as described in the text.

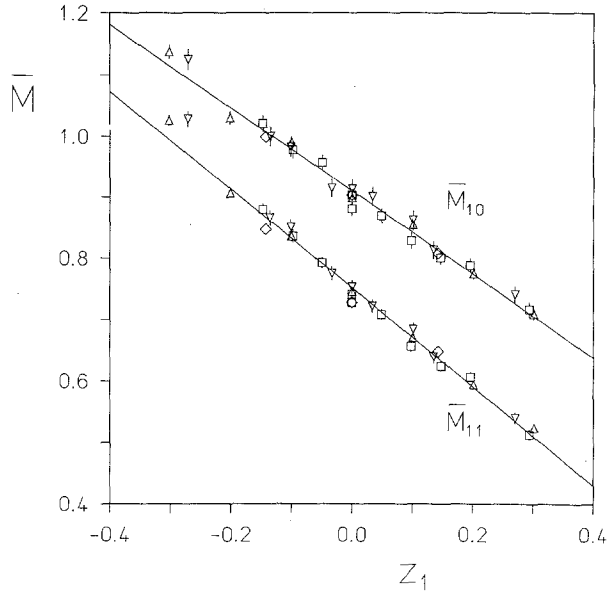

Fig. 14. Plots of $\bar{M}_{10}(z_1)$ and $\bar{M}_{11}(z_1)$ at $T=T_c$ as a function of z_1 for various L. The fit using a linear z_1 dependence represented by the lines includes $\Delta\eta$ as a free parameter (the form factor is set to 1).

From Table III we see that (4.14) agrees with the determination of ref. 3 inside 2 standard deviations.

There are two reasons which explain the gain in accuracy of J_{1c}, ϕ/ν, and $\Delta\eta$ by similar or less computational effort in comparison with ref. 3. First we use improved observables which are more sensitive to scaling and second the L dependence within FSS occurs not only in scaling factors like $L^{-\Delta\eta}$, but also in the argument z_1. The latter property is lost at the ordinary transition, where J_1 ceases to be a relevant variable. In order to determine β_1^o we have to study the moments as a function of L and T. We expect for γ defined as

$$\gamma = \frac{M_{21}(\theta_{2p})}{M_{20}(\theta_{2p})} = \frac{V}{A}\frac{\langle t\theta_{2p}\rangle}{\langle s\theta_{2p}} \tag{4.15}$$

the following scaling law:

$$\gamma = \left|1 - \frac{T}{T_c}\right|^{\beta-\beta_1^o} \bar{\gamma}(z) \tag{4.16}$$

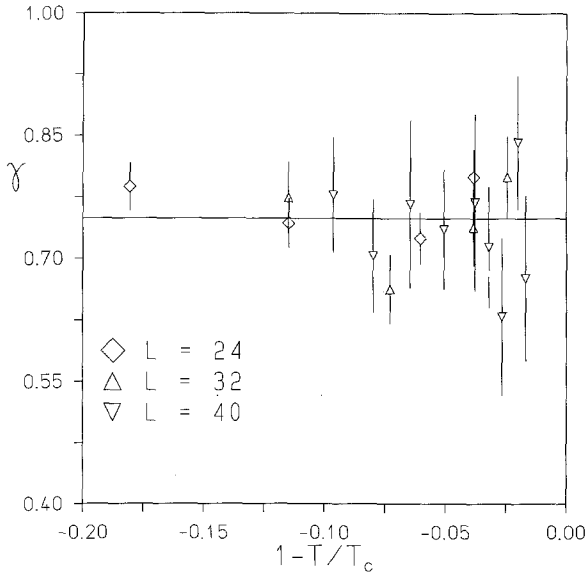

Fig. 15. Plot of $\bar{\gamma}$ defined in (4.16) as a function of $1-T/T_c$ at $J_1=0.5J$ for various L. The fit with a constant $\bar{\gamma}$ includes $\beta_1^c-\beta$ as a free parameter.

Our sample of data does not allow us to detect more than a constant behavior of the scaling function $\bar{\gamma}$. In Fig. 15 we show $\gamma|1-T/T_c|^{\beta_1^o-1}$ as a function of $1-T/T_c$ in the ordered phase at $J_1=0.5J$. The data are compatible with a constant $\bar{\gamma}$, which has been determined together with $\beta_1^o-\beta$ by a fit. This gives

$$\beta_1^o-\beta=0.421(22) \tag{4.17}$$

Since γ approaches the ratio of the order parameters m_1/m for $L\to\infty$ (see Appendix), the constant value $\bar{\gamma}$ can be taken as an estimate of the amplitude ratio

$$\left.\frac{B_1}{B}\right|_{J_1=0.5J}=0.77(5) \tag{4.18}$$

Both critical index (4.17) and the amplitude ratio (4.18) agree with the result of ref. 3.

5. CONCLUDING REMARKS

Our method employs clusters with nontrivial topological properties to extract critical parameters, assuming that moments have a scaling dimen-

sion independent of the loop number. The method has been tested successfully in models with periodic boundary conditions. In particular, the value for the critical temperature in the $d=3$ Ising model has an accuracy comparable to the series expansion of ref. 24 (see Table I). It agrees within 2 standard deviations with the more accurate values from Monte Carlo renormalization group methods[25] or the histogram method.[27] Our new results refer to the critical parameters related to the $d=3$ Ising model embedded in film geometry. Table III gives the comparison of our values with the results of ref. 3. The critical coupling (J_{1c}/J) and the magnetic index β_1^o agree, whereas we encounter a disagreement of 2–3 standard deviations for ϕ/ν and β_1^m. Both methods are difficult to compare, since we work exclusively at $T=T_c$ using FSS, and in ref. 3 the T dependence of the infinite lattice is employed. The lattice sizes are similar $(L \leqslant 40)$ in either case, whereas the type of possible scaling violations differs. We use multiplicative form factors, which cannot be represented by a shift of the critical temperature made in ref. 3. An answer probably requires a study of substantially larger lattice sizes.

Our results can be compared with the ε-expansion[1] (see Table III). For β_1^o or β_1^m the ε-expansion shows some kind of convergence and we find good agreement. Since the ε-expansion, the disagreement with our value should not be taken too seriously.

Our method uses FSS at the bulk critical temperature. Therefore determination of the amplitudes is impossible. Moments as functions of T have to be studied. In the ordered phase the problem is aggravated by the necessarity to subtract the corresponding combinations of order parameters (see Appendix). We hope to return to these questions in a separate publication.[28]

APPENDIX. SUSCEPTIBILITIES AND MOMENTS

To derive the relation between moments and susceptibilities χ, we start with the two-point function

$$g(x, y) = \langle \sigma_x \sigma_y \rangle \tag{A1}$$

Evaluating the r.h.s. in the SW algorithm, we have

$$g(x, y) = \left\{ \sum_{c,c'} \sigma_c \sigma_{c'} \Delta_c(x) \Delta_{c'}(y) \right\} \tag{A2}$$

where

$$\Delta_c(x) = \begin{cases} 1 & x \in c \\ 0 & \text{otherwise} \end{cases} \tag{A3}$$

Since spins in different clusters are independent, only the terms with $c = c'$ survive:

$$g(x, y) = \left\{ \sum_c \Delta_c(x)\, \Delta_c(y) \right\} \tag{A4}$$

The various susceptibilities in the disordered phase are sums over x, y in the bulk and/or in the surface. The bulk susceptibility is given by

$$\chi = \frac{1}{V} \sum_{x,y} g(x, y) = \frac{1}{V} \left\{ \sum_c s_c^2 \right\} = V M_{20}(1) \tag{A5}$$

The surface susceptibility χ_{11} and the mixed susceptibility χ_1 are given by

$$\chi_{11} = \frac{1}{A} \sum_{x,y \in A} g(x, y) = \frac{1}{A} \left\{ \sum_c t_c^2 \right\} = A M_{22}(1) \tag{A6}$$

and

$$\chi_1 = \frac{1}{A} \sum_{x \in V, y \in A} g(x, y) = \frac{1}{A} \left\{ \sum_c s_c t_c \right\} = V M_{21}(1) \tag{A7}$$

The cluster moments are averages over positive number in contrast to averages over $\sigma_x \sigma_y$ which have both signs. As a result the variance of $V M_{20}$ is much smaller than the variance of $(1/V)(\sum_x \sigma_x)^2$. For example, in the limit $T \to \infty$ we find $\Delta^2((\sum \sigma_x)^2/V) = 2$, whereas $\Delta^2(\sum_c s_c^2/V) \sim J/T$. In the ordered phase the unsubtracted susceptibilities (A5)–(A7) diverge with $L \to \infty$ with a constant M_{nm}. From this divergent part the order parameters can be estimated as

$$\lim_{L \to \infty} M_{k,l} = (m)^{k-l} (m_1)^l \tag{A8}$$

For a dimensionless SW distribution we see that m determined by

$$m^2 = \lim_{L \to \infty} \left\{ \sum_c \left(\frac{s_c}{V} \right)^2 \right\} \simeq \left\{ \Theta_d \left(\frac{s}{V} \right)^2 \right\} \tag{A9}$$

has the same dimension as the percolation order parameter m_p.

ACKNOWLEDGMENTS

We thank the Deutsche Forschungsgemeinschaft (C.R.) and the Studienstiftung des Deutschen Volkes (S.D.) for financial support. Computing time on a CRAY YMP was provided by HLRZ at Jülich. We are also grateful to Prof. K. Binder for valuable remarks and to Prof. S. Dietrich for illuminating discussions.

REFERENCES

1. H. W. Diehl, in *Phase Transitions and Critical Phenomena*, Vol. 10, C. Domb and J. Lebowitz, eds. (Academic Press, London, 1986).
2. K. Binder and P. C. Hohenberg, *Phys. Rev. B* **6**:3461 (1972); **9**:2194 (1974).
3. D. P. Landau and K. Binder, *Phys. Rev. B* **41**:4633 (1990).
4. M. Kikuchi and Y. Okabe, *Prog. Theor. Phys.* **73**:32 (1985).
5. K. Binder, in *Phase Transitions and Critical Phenomena*, Vol. 3, C. Domb and M. S. Green, eds. (Academic Press, London, 1976), p. 1.
6. R. H. Swendsen and J. S. Wang, *Phys. Rev. Lett.* **58**:86 (1987).
7. U. Wolff, *Phys. Rev. Lett.* **62**:361 (1989).
8. M. D. De Meo, D. W. Heermann, and K. Binder, *J. Stat. Phys.* **60**:585 (1990).
9. C. Ruge and F. Wagner, *J. Stat. Phys.* **66**:99 (1992).
10. P. J. Reynolds, H. E. Stanley, and W. Klein, *Phys. Rev. B* **21**:1223 (1980).
11. K. Binder, *Z. Phys. B* **43**:119 (1981).
12. P. W. Kasteleyn and C. M. Fortuin, *Phys. Soc. Jpn.* **26**(suppl.):11 (1969).
13. C. Domb, in *Phase Transitions and Critical Phenomena*, Vol. 3, C. Domb and M. S. Green, eds. (Academic Press, London, 1974), p. 357.
14. C. Ruge, S. Dunkelmann, and F. Wagner, *Phys. Rev. Lett.* **69**:2465 (1992).
15. F. T. Wu, *Rev. Mod. Phys.* **54**:235 (1982).
16. U. Wolff, *Nucl. Phys. B* **300** [FS22]:501 (1988).
17. L. de Arcangelis, *J. Phys. A* **20**:3057 (1987).
18. Stauffer, *Introduction to Percolation Theory* (Taylor & Francis, 1985).
19. J. Hoshen and R. Kopelman, *Phys. Rev. B* **27**:3438 (1976).
20. P. L. Leath, *Phys. Rev. B* **14**:5046 (1976).
21. J. S. Wang and R. H. Swendsen, *Physica A* **167**:567 (1990).
22. P. Tamajo, R. C. Brower, and W. Klein, *J. Stat. Phys.* **60**:889 (1990).
23. U. Wolff, *Nucl. Phys. B* **334**:581 (1990).
24. A. Liu and M. E. Fisher, *Physica A* **156**:35 (1989).
25. G. S. Pawley, R. H. Swendsen, D. J. Wallace, and K. G. Wilson, *Phys. Rev. B* **29**:4030 (1984).
26. C. F. Baillie, R. Gupta, K. A. Hawick, and C. S. Pawley, *Phys. Rev. B* **45**:10438 (1992).
27. A. M. Ferrenberg and D. P. Landau, *Phys. Rev. B* **44**:5081 (1991).
28. C. Ruge, S. Dunkelmann, F. Wagner, and J. Wulf, to be published.